Derivation of a single-band model for CuO_2 planes by a cell-perturbation method

J. H. Jefferson
DRA Electronics Division (Royal Signals and Radar Establishment), St. Andrews Road, Great Malvern, Worcestershire WR14 3PS, England

H. Eskes
Materials Science Centre, Department of Solid State and Applied Physics, University of Groningen, Nijenborgh 18, 9747 AG Groningen, The Netherlands

L. F. Feiner
Philips Research Laboratories, P. O. Box 80000, 5600 JA Eindhoven, The Netherlands

(Received 29 October 1991)

A cell-perturbation method is developed for CuO_2 planes in the cuprate superconductors described by a d-p model. It is shown that a single-band t-t'-J-J' model accurately describes the low-energy physics and how the parameters of this model vary with those of the underlying d-p model. The method is similar in spirit to Anderson's original treatment of superexchange [Phys. Rev. **115**, 2 (1959)], where the exchange interaction is obtained in second order rather than given by the usual fourth-order result of ordinary perturbation theory (a poor approximation). It is shown that O-O hopping can appreciably affect the absolute and relative magnitudes of the effective single-band parameters and that a regime with $J \sim t$ is quite conceivable. Although triplet (intermediate) states can appreciably enhance the magnitude of the "diagonal" effective hopping t', an effective single-band description should remain valid for all reasonable estimates of the underlying d-p parameters. Correction terms involving hole pairs on neighboring cells are derived and shown to be small. For the "undoped" case, an estimate is made of the critical charge-transfer energy for an insulator-metal transition.

I. INTRODUCTION

There has been considerable interest recently in the use of effective single-band models to describe charge-spin interactions in the CuO_2 planes of cuprate superconductors. This follows the pioneering suggestion by Anderson[1] that a simple spin-$\frac{1}{2}$ Hubbard Hamiltonian should model the essential physics. Since we are in the strong correlation regime ($U/t \gg 1$) then, to second order in t, the Hubbard model is equivalent to the so-called t-J model with $J = 4t^2/U$.[2]

The use of an effective single-band model has been questioned by a number of authors starting with Emery[3] who suggested that an extended Hubbard model, which includes orbitals on oxygen ($2p$) as well as copper ($3d$), should be used. It is now widely accepted that such a model (or, rather, class of models, depending on which p and d orbitals are retained) probably contains the essential physics as regards electronic properties over a wide range of energies from meV to tens of eV. Indeed, such models have been rather successful in interpreting a number of experiments on cuprate materials in general, particularly at the high-energy end, such as x-ray photoemission spectroscopy (XPS), electron energy-loss spectroscopy (EELS), etc.[4-9] These models have become known simply as "d-p" models or sometimes just the d-p model when only $3d_{x^2-y^2}$ orbitals on Cu and σ-bonded p_x (p_y) orbitals on oxygen are retained. Their justification has not only been through agreement with experiment but also on theoretical grounds where detailed constrained density-functional calculations have yielded estimates of the parameters of the model which are quantitatively consistent with those of experiment.[10,11] Although there is some variation of these estimates, such uncertainties are not too critical for many purposes and, in particular, the main results of this paper. A possible exception is the parameter ε, the so-called (bare) charge-transfer energy, which is difficult to estimate both theoretically and experimentally, there being estimates ranging from ~ 1 to ~ 5 eV. As we shall see, the parameters which we calculate (superexchange and effective hopping) vary rather rapidly with ε when it is small.

What is the relationship between the Hubbard model (or t-J model) and the d-p model? Under what conditions, if any, are they equivalent for the low-energy physics? These have been, and to some extent remain, controversial questions. It is not difficult to show that when the charge transfer (ε) and the Cu-Cu Coulomb repulsion (U_d) are the largest energies in the model the Hubbard and d-p models are equivalent. (See, for example, Ref. 12). However, this is surely not the case for cuprate superconductors. Anderson has always maintained their essential equivalence for the low-energy physics and this view was supported by the work of Zhang and Rice,[13] who showed that in certain circumstances (namely, sufficiently large charge-transfer energy and zero oxygen bandwidth) the d-p and t-J models are essentially equivalent at low energies. Further support has been given by numerical studies which show that the low-energy spectrum of a d-p model does, in some cir-

cumstances, resemble that of an effective single-band (t-J) model.[14–16] However, these results are not conclusive, since it is difficult to estimate corrections and also what form any such corrections would take in an effective Hamiltonian. Furthermore, Emery and Reiter[17] have given examples of where the two models give quite different behavior that cannot be explained by an effective single band and the matter remains controversial. In this paper we reexamine the problem by a cell-perturbation method which includes the effect of finite oxygen bandwidth, extending earlier work.[18] We show that this method yields accurate results over the whole range of parameters of interest. These results support the effective single-band picture and show that the most important corrections are due to triplet states with one hole on copper and one on oxygen (as conjectured by Emery and Reiter[17]). However, these corrections are still quite small, can be accounted for perturbatively, and in our view do not invalidate the reduction to an effective single-band model for realistic estimates of the parameters.

The layout of the paper is as follows. In Sec. II we describe briefly the cell-perturbation method. The basic model is defined in Sec. III and expressed in terms of exact eigenstates of overlapping CuO_4 cells. In Sec. IV we consider the insulating case in which there is, on average, one hole per cell. This is shown to be equivalent to a Heisenberg model by second-order perturbation theory. The variation of the nearest-neighbor exchange term with the underlying d-p parameters is shown to be substantially different from the usual fourth-order perturbation expression for superexchange. The conducting or "doped" case is consider in Sec. V where the reduction to a single-band model is derived. This is a t-t'-J-J' model when only terms up to next-nearest neighbor are retained (longer range terms are much smaller). Comparison is made with exact results on finite clusters in Sec. VI where it is shown that our cell-perturbation method is very accurate over the parameter range of interest. By comparison, the usual perturbation results are shown to be rather poor. Corrections are considered in Sec. VII where it is shown that the most important ones are due to triplet (intermediate) states which have the effect of renormalizing the next-nearest-neighbor hopping parameter (t') as well as giving rise to small spin-dependent hopping terms. Hole pairs on adjacent cells give rise to an attractive interaction but this is relatively small and almost certainly swamped by kinetic-energy effects. Finally in Sec. VIII we discuss the results and point out that although the method is convergent, even when $\varepsilon \sim 0$, an insulator-metal (Mott) transition must take place in the case of one hole per cell and the critical charge-transfer gap at which this occurs is estimated.

II. THE CELL-PERTURBATION METHOD

The basic idea behind the cell-perturbation method is to perform a spatial decomposition of an interacting electron system into a network of equivalent cells. These cells may be overlapping, though this is not usually the case. A simple example is the decomposition of a crystal into atoms or molecules. The advantage of such a cell decimation is that it has the capability of treating local correlations to arbitrary accuracy, a fact recognized by Hubbard in the second of his classic series of papers on the subject.[19] This is also the motivation behind the numerical renormalization-group method in which the spatial decomposition is done in a hierarchical fashion with ever increasing cell sizes.[20] A further application is to magnetic insulators where such a localized description leads to effective spin Hamiltonians.[21] In all these cases the procedure is basically the same. We first choose a localized one-electron basis set in which each orbital has a label referring to its "parent" cell centered at $\mathbf{r}$. The particular choice will depend on the problem under consideration but, in general, it is always possible to choose an orthonormal set, even when the cells are overlapping (see Sec. III for a specific case of this). In principle one can work with nonorthogonal orbitals[22] though this leads to mathematical difficulties which, for our purposes, are best avoided. The Hamiltonian expressed in this localized basis may be written

$$H = H_0 + H_1 \ , \tag{1}$$

where

$$H_0 = \sum_{\mathbf{r}} h_{0\mathbf{r}}$$

and

$$H_1 = \sum_{\substack{\mathbf{r},\mathbf{r}' \\ (\mathbf{r}\neq\mathbf{r}')}} v_{\mathbf{r},\mathbf{r}'} \ .$$

The "cell-Hamiltonian," $h_{0\mathbf{r}}$, is that part of H which only involves orbitals associated with the cell located at $\mathbf{r}$, whereas $v_{\mathbf{r},\mathbf{r}'}$ are the interaction terms associated with cells at $\mathbf{r}$ and $\mathbf{r}'$.

The next step is to express the Hamiltonian in terms of the eigenstates of the cells, i.e., we solve the (few-electron) Schrödinger equation

$$h_0|\nu\rangle = \varepsilon_\nu|\nu\rangle$$

for one cell exactly (or to any desired accuracy) and then express the Hamiltonian in this basis set, i.e.,

$$H = \sum_{\mathbf{r},\nu} \varepsilon_\nu X^{\mathbf{r}}_{\nu\nu} + \sum_{\substack{\mathbf{r},\nu,\nu' \\ \mathbf{r}',\mu,\mu'}} \langle \mathbf{r}\nu'\mathbf{r}'\mu'|v_{\mathbf{r}\mathbf{r}'}|\mathbf{r}\nu\mathbf{r}'\mu\rangle X^{\mathbf{r}}_{\nu'\nu} X^{\mathbf{r}'}_{\mu'\mu} \ , \tag{2}$$

where $X^{\mathbf{r}}_{\nu'\nu} = |\mathbf{r}\nu'\rangle\langle\mathbf{r}\nu|$ are projection operators, using the notation of Hubbard.[19] In these expressions ν denotes collectively a complete set of quantum numbers for a single cell, including n, the number of electrons. It should also be noted that the two-cell matrix elements, $\langle \mathbf{r}\nu'\mathbf{r}'\mu'|v_{\mathbf{r}\mathbf{r}'}|\mathbf{r}\nu\mathbf{r}'\mu\rangle$, depend only on the separation between the cells, $|\mathbf{r}-\mathbf{r}'|$.

Thus far we have not made any approximation but have merely expressed the Hamiltonian in a new basis. To make further progress we reduce the size of the Hilbert space by generating an effective Hamiltonian using Rayleigh-Schrödinger perturbation theory as follows. H_0

is diagonal in the cell basis and, for the cases of interest, there will be a large degeneracy associated with its ground state. For example, if each cell has ground-state energy ε_0 and associated degeneracy d_0 then H_0 has ground-state energy $N\varepsilon_0$ and is d_0^N-fold degenerate for N cells. These d_0^N states will evolve into exact eigenstates of H when the cell-cell interaction H_1 is "switched on." It may be shown[23,24] that these eigenstates of H may be determined from an "effective" Schrödinger equation

$$H_{\text{eff}}|\Phi\rangle = E|\Phi\rangle \ ,$$

where E is a true eigenenergy of H. H_{eff} is given explicitly by the Rayleigh-Schrödinger expansion

$$H_{\text{eff}} = P_0 \left[H + H_1 \frac{(1-P_0)}{E_0 - H_0} H_1 + \cdots \right] P_0 \ , \tag{3}$$

where P_0 is the projection operator for the ground manifold of H_0. Furthermore, the true eigenstate $|\Psi\rangle$ of H is given by the Rayleigh-Schrödinger expansion

$$|\Psi\rangle = \left[1 + \frac{(1-P_0)}{E_0 - H_0} H_1 + \cdots \right] |\Phi\rangle \ . \tag{4}$$

In practice, of course, the Rayleigh-Schrödinger expansions must be truncated and the method is most useful when there is rapid convergence. This is indeed the case for the problem of CuO_2 planes and we will show that second-order results are very accurate for the parameters of interest.

The usefulness of the cell-perturbation method in general lies in the fact that H_{eff} belongs to a smaller Hilbert space than the original Hamiltonian, which has obvious computational advantage for finite clusters. Furthermore, the effective Hamiltonian can sometimes be written in a simple form, or mapped on to a related problem, thereby giving further insight into possible low-energy solutions.

III. THE BASIC HAMILTONIAN

Let us now apply the general method outlined in Sec. II to a single CuO_2 plane. We start with the so-called d-p model or extended Hubbard model.[3] The Hamiltonian is

$$\begin{aligned} H = \sum_{\mathbf{r}\sigma} & (\varepsilon_d n^{(d)}_{\mathbf{r},\sigma} + \varepsilon_p (n^{(p)}_{\mathbf{r},\mathbf{x},\sigma} + n^{(p)}_{\mathbf{r},\mathbf{y},\sigma}) + t_{pd}[d^\dagger_{\mathbf{r},\sigma}(-p_{\mathbf{r},\mathbf{x},\sigma} + p_{\mathbf{r},\mathbf{y},\sigma} + p_{\mathbf{r},-\mathbf{x},\sigma} - p_{\mathbf{r},-\mathbf{y},\sigma}) + \text{H.c.}] \\ & + t_{pp}(p^\dagger_{\mathbf{r},\mathbf{y},\sigma} p_{\mathbf{r},\mathbf{x},\sigma} + p^\dagger_{\mathbf{r},-\mathbf{y},\sigma} p_{\mathbf{r},-\mathbf{x},\sigma} - p^\dagger_{\mathbf{r},\mathbf{y},\sigma} p_{\mathbf{r},-\mathbf{x},\sigma} - p^\dagger_{\mathbf{r},-\mathbf{y},\sigma} p_{\mathbf{r},\mathbf{x},\sigma} + \text{H.c.}) \\ & + \tfrac{1}{2} U_d n^{(d)}_{\mathbf{r},\sigma} n^{(d)}_{\mathbf{r},-\sigma} + \tfrac{1}{2} U_p (n^{(p)}_{\mathbf{r},\mathbf{x},\sigma} n^{(p)}_{\mathbf{r},\mathbf{x},-\sigma} + n^{(p)}_{\mathbf{r},\mathbf{y},\sigma} n^{(p)}_{\mathbf{r},\mathbf{y},-\sigma})) \ . \end{aligned} \tag{5}$$

In this Hamiltonian, $d^\dagger_{\mathbf{r},\sigma}$ creates a hole in a $3d_{x^2-y^2}$ orbital at Cu site $\mathbf{r}$, whereas $p^\dagger_{\mathbf{r},\mathbf{x},\sigma}$ creates a hole in a p_x orbital at oxygen site $\mathbf{r}+\frac{1}{2}\mathbf{x}$, where $\mathbf{x}$ is a Cu-Cu lattice parameter in the x direction (and similarly for $p^\dagger_{\mathbf{r},\mathbf{y},\sigma}$). ε_p and ε_d are the energies of the localized holes. We have used a phase convention such that orbitals on each CuO_2 cell transform in the same way, with p_x (p_y) transforming like x (y).

The largest energy parameter is U_d, the Coulomb repulsion between two holes on the same Cu site. In what follows we shall set $U_d = \infty$ and neglect the corresponding U_p for the oxygen sites. Whilst this is not essential, it is convenient since it enables us to obtain a number of analytic results which would otherwise not be possible. It is quite straightforward to generalize these results to finite U_p and U_d by purely numerical means though this is not expected to make any significant changes. (The main effect will be to renormalize the parameters of the effective single-band Hamiltonian, which we will derive below.) With these simplifications the Hamiltonian may be written

$$\begin{aligned} H = P \Bigg[& \sum_{\mathbf{r},\sigma} \varepsilon (n^{(p)}_{\mathbf{r},\mathbf{x},\sigma} + n^{(p)}_{\mathbf{r},\mathbf{y},\sigma}) + t_{pd}[d^\dagger_{\mathbf{r},\sigma}(-p_{\mathbf{r},\mathbf{x},\sigma} + p_{\mathbf{r},\mathbf{y},\sigma} + p_{\mathbf{r},-\mathbf{x},\sigma} - p_{\mathbf{r},-\mathbf{y},\sigma}) + \text{H.c.}] \\ & + t_{pp}(p^\dagger_{\mathbf{r},\mathbf{y},\sigma} p_{\mathbf{r},\mathbf{x},\sigma} + p^\dagger_{\mathbf{r},-\mathbf{y},\sigma} p_{\mathbf{r},-\mathbf{x},\sigma} - p^\dagger_{\mathbf{r},\mathbf{y},\sigma} p_{\mathbf{r},-\mathbf{x},\sigma} - p^\dagger_{\mathbf{r},-\mathbf{y},\sigma} p_{\mathbf{r},\mathbf{x},\sigma} + \text{H.c.}) \Bigg] P \ , \end{aligned} \tag{6}$$

where P is a projection operator that ensures that no double occupation of the Cu sites can occur. [Formally, $P = \prod_{\mathbf{r}} (1 + n^{(d)}_{\mathbf{r}})(1 - \frac{1}{2} n^{(d)}_{\mathbf{r}})$.] $\varepsilon = \varepsilon_p - \varepsilon_d$ (the charge-transfer energy) and the constant energy term $\varepsilon_d \sum_{\mathbf{r}} [n^{(d)}_{\mathbf{r}} + n^{(p)}_{\mathbf{r},\mathbf{x}} + n^{(p)}_{\mathbf{r},\mathbf{y}}] = \varepsilon_d N_h$ has been dropped.

Following Zhang and Rice[13] we divide the CuO_2 plane into overlapping CuO_4 cells as shown in Fig. 1. The oxygen p orbitals may now be replaced by independent linear combinations centered on each copper site. There are, of course, only two independent combinations for each Cu site (cell) which may be chosen to be the combinations $p_{\mathbf{r},\mathbf{x},\sigma} - p_{\mathbf{r},\mathbf{y},\sigma} - p_{\mathbf{r},-\mathbf{x},\sigma} + p_{\mathbf{r},-\mathbf{y},\sigma}$ and $p_{\mathbf{r},\mathbf{x},\sigma} + p_{\mathbf{r},\mathbf{y},\sigma} - p_{\mathbf{r},-\mathbf{x},\sigma} - p_{\mathbf{r},-\mathbf{y},\sigma}$. These states are not orthogonal since adjacent cells have a common bridging oxygen but may be orthogonalized by forming Wannier functions. Althernatively and equivalently we can, following Shastry,[25] first express the p orbitals in the Bloch basis and then transform to "canonical fermions"

$$\alpha_{\mathbf{k},\sigma} = i(s_{\mathbf{k},\mathbf{x}} p_{\mathbf{k},\mathbf{x},\sigma} - s_{\mathbf{k},\mathbf{y}} p_{\mathbf{k},\mathbf{y},\sigma})/\mu_{\mathbf{k}}$$

and

$$\beta_{\mathbf{k},\sigma}=-i(s_{\mathbf{k},\mathrm{y}}p_{\mathbf{k},\mathrm{x},\sigma}+s_{\mathbf{k},\mathrm{x}}p_{\mathbf{k},\mathrm{y},\sigma})/\mu_{\mathbf{k}} ,$$

where $s_{\mathbf{k},\mathrm{x}}=\sin\frac{1}{2}\mathbf{k}\cdot\mathbf{x}$, $s_{\mathbf{k},\mathrm{y}}=\sin\frac{1}{2}\mathbf{k}\cdot\mathbf{y}$, and $\mu_{\mathbf{k}}^2=(s_{\mathbf{k},\mathrm{x}}^2+s_{\mathbf{k},\mathrm{y}}^2)$. Substituting these definitions into Eq. (6) and Fourier transforming back into real space gives

$$H=P\left[\varepsilon\sum_{\mathrm{r},\sigma}(\alpha_{\mathrm{r},\sigma}^{\dagger}\alpha_{\mathrm{r},\sigma}+\beta_{\mathrm{r},\sigma}^{\dagger}\beta_{\mathrm{r},\sigma})-2t_{pd}\sum_{\mathrm{r},\mathrm{r}',\sigma}\mu(\mathbf{r}-\mathbf{r}')(d_{\mathrm{r},\sigma}^{\dagger}\alpha_{\mathrm{r}',\sigma}+\mathrm{H.c.})\right.$$
$$\left.-2t_{pp}\sum_{\mathrm{r},\mathrm{r}',\sigma}[\nu(\mathbf{r}-\mathbf{r}')(\alpha_{\mathrm{r},\sigma}^{\dagger}\alpha_{\mathrm{r}',\sigma}-\beta_{\mathrm{r},\sigma}^{\dagger}\beta_{\mathrm{r}',\sigma})+\chi(\mathbf{r}-\mathbf{r}')(\alpha_{\mathrm{r},\sigma}^{\dagger}\beta_{\mathrm{r}',\sigma}+\mathrm{H.c.})]\right]P , \quad (7)$$

where

$$\mu(\mathbf{r})=N^{-1}\sum_{\mathbf{k}}e^{-i\mathbf{k}\cdot\mathbf{r}}\mu_{\mathbf{k}} ,$$

$$\nu(\mathbf{r})=N^{-1}\sum_{\mathbf{k}}e^{-i\mathbf{k}\cdot\mathbf{r}}(2s_{\mathbf{k},\mathrm{x}}s_{\mathbf{k}\mathrm{y}}/\mu_{\mathbf{k}})^2 ,$$

and

$$\chi(\mathbf{r})=N^{-1}\sum_{\mathbf{k}}e^{-i\mathbf{k}\cdot\mathbf{r}}\frac{2(s_{\mathbf{k},\mathrm{x}}^2-s_{\mathbf{k},\mathrm{y}}^2)s_{\mathbf{k},\mathrm{x}}s_{\mathbf{k}\mathrm{y}}}{\mu_{\mathbf{k}}^2} .$$

The first few of these coupling constants are shown below in Table I for an infinite plane (where we have set the Cu-Cu lattice parameter to unity). They are seen to fall off rapidly with distance and we shall only retain up to next-nearest-neighbor terms. It is also a very good approximation to drop the χ term mixing the α and β orbitals. This can be seen by comparing the exact result for $t_{pd}=0$ (oxygen bands only) with the approximate result in which the $\alpha-\beta$ mixing is neglected. The exact energy dispersion for the oxygen bands is $\pm 4t_{pp}s_{\mathbf{k},\mathrm{x}}s_{\mathbf{k},\mathrm{y}}$, whereas the dispersion of the α and β states is [from the t_{pp} term in Eq. (7)] $\pm 8t_{pp}s_{\mathbf{k},\mathrm{x}}^2s_{\mathbf{k},\mathrm{y}}^2/(s_{\mathbf{k},\mathrm{x}}^2+s_{\mathbf{k},\mathrm{y}}^2)$. These energy dispersions are shown in Fig. 2 along the direction $(\pi,0)$ to $\pi,\pi)$ and we see that the approximate dispersion $[\chi(\mathbf{r})=0]$ is very accurate close to the band minimum, which is the region of interest. With the mixing of the α and β orbitals neglected the β terms decouple (since only the α orbitals hybridize with the d orbitals) and hence may be dropped. (However, it should be noted that for a sufficiently large number of holes the β band will become occupied. We shall only consider the case of "low doping" in this paper.) The Hamiltonian (7) then simplifies to

$$H=H_0+H_1 ,$$

where

$$H_0=\sum_{\mathrm{r},\sigma}P[\bar{\varepsilon}n_{\mathrm{r},\sigma}^{(\alpha)}+\tau_0(d_{\mathrm{r},\sigma}^{\dagger}\alpha_{\mathrm{r}',\sigma}+\mathrm{H.c.})]P$$

is the on-site Hamiltonian with $\bar{\varepsilon}=\varepsilon-2t_{pp}\nu(\mathbf{0})$ and $\tau_0=-2t_{pd}\mu(\mathbf{0})$. Similarly, for the interactions between neighboring sites

$$H_1=\sum_{\substack{\mathrm{r},\mathrm{r}'\\(\mathbf{r}\neq\mathbf{r}')}}P[\tau(\mathbf{r}-\mathbf{r}')(d_{\mathrm{r},\sigma}^{\dagger}\alpha_{\mathrm{r}',\sigma}+\mathrm{H.c.})$$
$$+\tau'(\mathbf{r}-\mathbf{r}')\alpha_{\mathrm{r},\sigma}^{\dagger}\alpha_{\mathrm{r}',\sigma}]P , \quad (8)$$

where $\tau(\mathbf{r}-\mathbf{r}')=-2t_{pd}\mu(\mathbf{r}-\mathbf{r}')$ and $\tau'(\mathbf{r}-\mathbf{r}')=-2t_{pp}\nu(\mathbf{r}-\mathbf{r}')$. We note that the Hamiltonian in this representation is of the general form given in Eq. (1) of Sec. II [as is Eq. (7)].

The on-site Hamiltonian, H_0, is easily diagonalized. For a cell with just one hole the single-particle base states are $|d_\sigma\rangle$ and $|\alpha_\sigma\rangle$, giving a Hamiltonian matrix

$$\begin{bmatrix}0 & \tau_0\\ \tau_0 & \bar{\varepsilon}\end{bmatrix} ,$$

with eigenvalues and eigenfunctions

$$e_{\pm}=\tfrac{1}{2}[\bar{\varepsilon}\pm(\bar{\varepsilon}^2+4\tau_0^2)^{1/2}] , \quad (9)$$

$$|\psi_{-}^{\sigma}\rangle=\cos\theta|d_\sigma\rangle+\sin\theta|\alpha_\sigma\rangle , \quad (10)$$

and

$$|\psi_{+}^{\sigma}\rangle=-\sin\theta|d_\sigma\rangle+\cos\theta|\alpha_\sigma\rangle \quad (11)$$

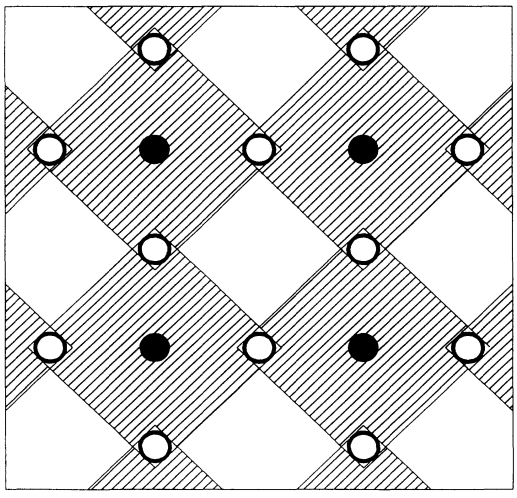

FIG. 1. Overlapping CuO_4 cells. ● Cu; ○ oxygen.

TABLE I. Values of the first few coupling constants (in units of the Cu-Cu lattice parameter).

$\lvert\mathbf{r}-\mathbf{r}'\rvert$	μ	ν	χ
0	0.958	0.727	0
1	−0.14	−0.273	−0.133
$\sqrt{2}$	−0.02	0.122	0
2	−0.02	−0.064	0.041

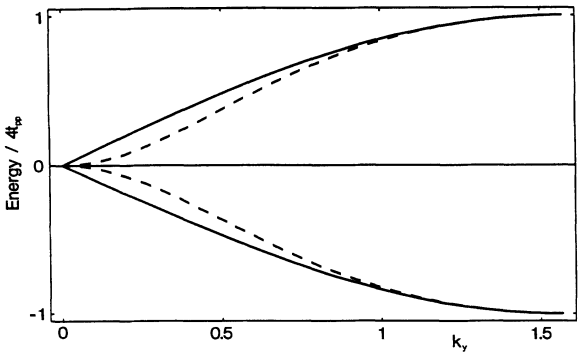

FIG. 2. Comparison of exact solution for oxygen bands (solid line) with α states only (dashed curve) along $(\pi,0)$ to (π,π).

with $\tan 2\theta = -2\tau_0/\bar{\varepsilon}$. Note that for $\tau_0 \ll \bar{\varepsilon}$ we recover the usual perturbation results: $|\psi_+^\sigma\rangle \simeq |\alpha_\sigma\rangle + (\tau_0/\bar{\varepsilon})|d_\sigma\rangle$ with $e_+ \simeq \bar{\varepsilon} + \tau_0^2/\bar{\varepsilon}$, and $|\psi_-^\sigma\rangle \simeq |d_\sigma\rangle - (\tau_0/\bar{\varepsilon})|\alpha_\sigma\rangle$ with $e_- \simeq -\tau_0^2/\bar{\varepsilon}$. However, since we are interested in cases for which $\tau_0 \sim \bar{\varepsilon}$ we shall not make this second-order approximation.

Similarly for two holes on a cell the single-cell base states are

$$|d,\alpha\rangle_s = \frac{|d_\uparrow,\alpha_\downarrow\rangle - |d_\downarrow,\alpha_\uparrow\rangle}{\sqrt{2}}, |\alpha_\uparrow,\alpha_\downarrow\rangle$$

for the singlet states and

$$|\psi_{1,-1}^t\rangle = |d_\downarrow,\alpha_\downarrow\rangle ,$$

$$|\psi_{1,0}^t\rangle = \frac{|d_\uparrow,\alpha_\downarrow\rangle + |d_\downarrow,\alpha_\uparrow\rangle}{\sqrt{2}} ,$$

$$|\psi_{1,1}^t\rangle = |d_\uparrow,\alpha_\uparrow\rangle$$

for the triplet states. The latter are also eigenstates since the α and d states are not mixed in the triplet manifold and the triplet energy is thus $\bar{\varepsilon}$. Note also that we have omitted the base state $|d_\uparrow,d_\downarrow\rangle$ because of the constraint $U_d = \infty$ (enforced by the projection operator P).

The singlet Hamiltonian matrix is

$$\begin{bmatrix} \bar{\varepsilon} & \sqrt{2}\tau_0 \\ \sqrt{2}\tau_0 & 2\bar{\varepsilon} \end{bmatrix}$$

with eigensolutions

$$E_\pm = \tfrac{1}{2}[3\varepsilon \pm (\bar{\varepsilon}^2 + 8\tau_0^2)^{1/2}] , \tag{12}$$

$$|\psi_-^s\rangle = \cos\phi|d,\alpha\rangle_s + \sin\phi|\alpha_\uparrow,\alpha_\downarrow\rangle , \tag{13}$$

and

$$|\psi_+^s\rangle = -\sin\phi|d,\alpha\rangle_s + \cos\phi|\alpha_\uparrow,\alpha_\downarrow\rangle , \tag{14}$$

with $\tan 2\phi = -2\sqrt{2}\tau_0/\bar{\varepsilon} = \sqrt{2}\tan\theta$.

Cell states with three or more holes are much higher in energy and will be neglected here. (They may, however, be important as intermediate states when hole pair-pair interactions on neighboring sites are considered. See Sec. VI.)

With the above eigenstates it is now straightforward to express the Hamiltonian in the form given by Eq. (2). For example, the cell-diagonal part of the Hamiltonian H_0 is

$$H_0 = \sum_{\mathbf{r}} [e_+ X_+^{\mathbf{r}} + e_- X_-^{\mathbf{r}} + E_+ X_{S_+}^{\mathbf{r}} + E_- X_{S_-}^{\mathbf{r}} + \bar{\varepsilon}(X_{1,-1}^{\mathbf{r}} + X_{1,0}^{\mathbf{r}} + X_{1,1}^{\mathbf{r}})] , \tag{15}$$

where we have set $X_{\nu\nu}^{\mathbf{r}} = X_\nu^{\mathbf{r}}$ and $\sum_\sigma X_{\pm\sigma} = X_\pm$ for brevity. In a similar fashion we could express the cell-cell interaction H_1 in the cell-eigenstate basis but, as we shall see, it is more convenient to leave it in terms of the one-electron basis, Eq. (8).

IV. THE INSULATING CASE

In the insulating case there is exactly one hole per CuO_2 cell (on average). If we neglect the cell-cell interaction, Eq. (8), then H_0 is diagonal in the cell basis [see Eq. (15)] and the ground manifold is 2^N-fold degenerate with energy $E_0 = Ne_-$, where N is the number of cells. Switching on the cell-cell hopping as a perturbation gives rise to an effective Hamiltonian operating in this ground manifold set of states $\{|\sigma_1,\sigma_2,\ldots,\sigma_N\rangle\}$ [where we have written $|\psi_-^\sigma\rangle = |\sigma\rangle$ for brevity, see Eq. (10)]. To second-order this effective Hamiltonian is given by Eq. (3) and we may write

$$\frac{1-P_0}{E_0 - H_0} = \sum_i \frac{|i\rangle\langle i|}{E_0 - E_i} ,$$

where the intermediate states $|i\rangle$ have one or more sites doubly occupied with holes. Note that $P_0 H_1 P_0 = 0$ since H_1 will always transfer a hole from one site to another and thus take us out of the ground manifold.

Examples of second-order hopping processes for nearest-neighbor cells are shown in Fig. 3 where the in-

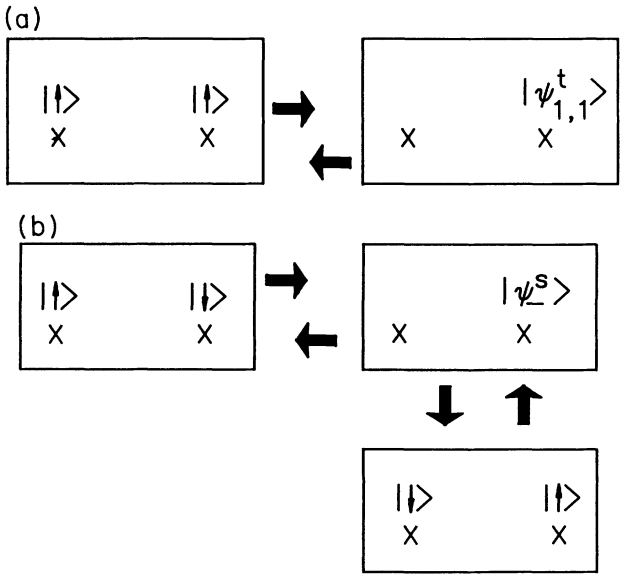

FIG. 3. Second-order hopping processes for nearest-neighbor cells ($X = CuO_4$ cell). (a) via a triplet. (b) via a singlet (includes spin exchange).

termediate two-hole states are those derived in Sec. III. Note that processes are allowed for adjacent spins both parallel [Fig. 3(a)] and antiparallel [Fig. 3(b)]. This should be contrasted with a single-band spin-$\frac{1}{2}$ model (such as the Hubbard model) where a spin may only hop to an adjacent site if it has the opposite spin because of the Pauli principle. However, we emphasize that, as with the single-band Hubbard model, this is a *second*-order calculation which, as we will show, gives rise to the usual (fourth-order) magnetic superexchange in a certain limit; though in general the present method is much more accurate. In this sense it is similar to Anderson's original treatment of transition-metal salts where the hybridization of the d electrons on a magnetic ion with the p orbitals on surrounding ligands is taken into account first and the superexchange is given in second order.[26] With this cell approach there are, of course, longer range hopping processes of exactly the same form but these fall off rapidly with distance.

Using these intermediate states in the second-order perturbation expression enables the effective Hamiltonian to be written in the form (dropping the constant $P_0H_0P_0=e_-\sum_{\mathbf{r}}X^{\mathbf{r}}_{-}=Ne_-P_0$)

$$H_{\text{eff}}=\sum_{\langle \mathbf{r},\mathbf{r}'\rangle,\sigma}[\Delta_1 X^{\mathbf{r}}_{\sigma,\sigma}X^{\mathbf{r}'}_{\sigma,\sigma}+(\tfrac{1}{2}\Delta_1+\Delta_2)X^{\mathbf{r}}_{\sigma,\sigma}X^{\mathbf{r}'}_{-\sigma,-\sigma} +(\tfrac{1}{2}\Delta_1-\Delta_2)X^{\mathbf{r}}_{-\sigma,\sigma}X^{\mathbf{r}'}_{\sigma,-\sigma}], \tag{16}$$

where

$$X^{\mathbf{r}}_{\sigma,\sigma'}=|\sigma_{\mathbf{r}}\rangle\langle\sigma'_{\mathbf{r}}|, \tag{17}$$

$$\Delta_1(\mathbf{R})=\frac{2|\langle\psi^t_{0,2\sigma},0|v(\mathbf{R})|\sigma,\sigma\rangle|^2}{\bar{e}-2e_-}, \tag{18}$$

$$\Delta_2(\mathbf{R})=-\frac{2|\langle\psi^s_+,0|v(\mathbf{R})|\uparrow,\downarrow\rangle|^2}{E_+-2e_-}-\frac{2|\langle\psi^s_-,0|v(\mathbf{R})|\uparrow,\downarrow\rangle|^2}{E_--2e_-}, \tag{19}$$

and $v(\mathbf{R})$ is that part of H_1 [Eq. (8)] referring to interactions between two cells only, located at $\mathbf{O}$ and $\mathbf{R}=\mathbf{r}-\mathbf{r}'$, i.e.,

$$v(\mathbf{R})=P[\tau(\mathbf{R})(d^\dagger_{0,\sigma}\alpha_{\mathbf{R},\sigma}+d^\dagger_{\mathbf{R},\sigma}\alpha_{0,\sigma}+\text{H.c.}) +\tau'(\mathbf{R})(\alpha^\dagger_{0,\sigma}\alpha_{\mathbf{R},\sigma}+\text{H.c.})]P . \tag{20}$$

In Eq. (16) the angular brackets denote summation over pairs of sites $\mathbf{r}$ and $\mathbf{r}'$ (not necessarily nearest neighbors), i.e., a pair is only counted once. In deriving this equation we have used the symmetry relations

$$\langle\psi^t_{1,0},0|v(\mathbf{R})|\uparrow,\downarrow\rangle=\langle\psi^t_{1,0},0|v(\mathbf{R})|\downarrow,\uparrow\rangle =\langle\psi^t_{1,2\sigma},0|v(\mathbf{R})|\sigma,\sigma\rangle/\sqrt{2}$$

and

$$\langle\psi^s_\pm,0|v(\mathbf{R})|\uparrow,\downarrow\rangle=-\langle\psi^s_\pm,0|v(\mathbf{R})|\downarrow,\uparrow\rangle .$$

Equation (16) can be simplified further using the identities

$$\sum_\sigma X^{\mathbf{r}}_{\sigma,\sigma}X^{\mathbf{r}'}_{\sigma,\sigma}=\tfrac{1}{2}+2s^z_{\mathbf{r}}s^z_{\mathbf{r}'}, \tag{21}$$

$$\sum_\sigma X^{\mathbf{r}}_{\sigma,\sigma}X^{\mathbf{r}'}_{-\sigma,-\sigma}=\tfrac{1}{2}-2s^z_{\mathbf{r}}s^z_{\mathbf{r}'}, \tag{22}$$

and

$$\sum_\sigma X^{\mathbf{r}}_{\sigma,-\sigma}X^{\mathbf{r}'}_{-\sigma,\sigma}=s^+_{\mathbf{r}}s^-_{\mathbf{r}'}+s^-_{\mathbf{r}}s^+_{\mathbf{r}'}=2(s^x_{\mathbf{r}}s^x_{\mathbf{r}'}+s^y_{\mathbf{r}}s^y_{\mathbf{r}'}) . \tag{23}$$

Substituting these relations into Eq. (16) and dropping a constant term gives

$$H_{\text{eff}}=\sum_{\langle\mathbf{r},\mathbf{r}'\rangle}J(\mathbf{r}-\mathbf{r}')\mathbf{s}_{\mathbf{r}}\cdot\mathbf{s}_{\mathbf{r}'}, \tag{24}$$

where $J=\Delta_1-2\Delta_2$. Hence, to second order in the cell-cell interaction, the effective Hamiltonian reduces to a Heisenberg model. Detailed calculation using Eqs. (9), (10), (12), (13), (18), and (19) gives

$$J(\mathbf{r}-\mathbf{r}')=\frac{[\tau(\mathbf{r}-\mathbf{r}')\cos(2\theta)+\frac{1}{2}\tau'(\mathbf{r}-\mathbf{r}')\sin(2\theta)]^2}{e_--\frac{1}{2}\bar{\varepsilon}} +\frac{\{\tau(\mathbf{r}-\mathbf{r}')[\sqrt{2}\cos\phi+\sin(2\theta)\sin\phi]+\tau'(\mathbf{r}-\mathbf{r}')(2\sin^2\theta\sin\phi+\frac{1}{\sqrt{2}}\sin\theta\cos\phi)\}^2}{E_--2e_-} . \tag{25}$$

In this expression the contribution that arises from intermediate states in which two holes form a singlet ψ^s_+ has been dropped since it has a large energy compared with the other singlet state ψ^s_- and the triplet states and is negligible.

We can examine the perturbation limit of J by expanding in powers of $t_{pd}/\bar{\varepsilon}$. This gives, to lowest order

$$J(\mathbf{r}-\mathbf{r}')=256\mu_0^2\mu(\mathbf{r}-\mathbf{r}')^2\left[1+\frac{\nu_0\nu(\mathbf{r}-\mathbf{r}')}{\mu(\mathbf{r}-\mathbf{r}')}\frac{t_{pp}}{\bar{\varepsilon}}\right] \times\left[1+2\frac{\nu_0\nu(\mathbf{r}-\mathbf{r}')}{\mu(\mathbf{r}-\mathbf{r}')}\frac{t_{pp}}{\bar{\varepsilon}}\right]\frac{t_{pd}^4}{\bar{\varepsilon}^3} . \tag{26}$$

Substituting the numerical values of the coupling constants for nearest-neighbor cells from Table I we get

$$J\simeq 4.6\left[1+1.87\frac{t_{pp}}{\bar{\varepsilon}}\right]\left[1+3.74\frac{t_{pp}}{\bar{\varepsilon}}\right]\frac{t_{pd}^4}{\bar{\varepsilon}^3} . \tag{27}$$

We see from these equations that one of the main effects of t_{pp} is to increase the superexchange by reducing the charge-transfer gap from ε to $\bar{\varepsilon}=\varepsilon-2\nu_0t_{pp}$, which is simply due to the kinetic energy of the oxygen hole around the CuO_4 cell. The usual fourth-order perturbation result for the superexchange with $t_{pp}=0$ and $U_d=\infty$ is $J=4t_{pd}^4/\varepsilon^3$ and for this case the expression (27) is in error

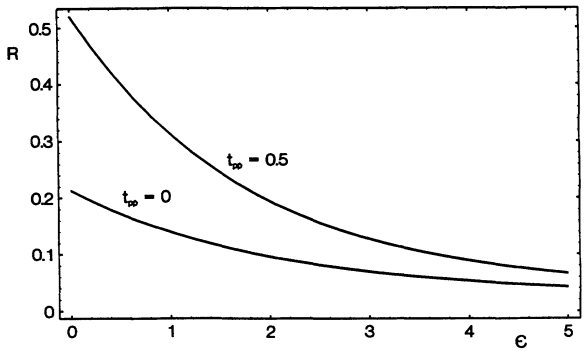

FIG. 4. Ratio of charge-transfer matrix element to energy required to make transfer vs p-d energy splitting (ε).

by 15%. The source of this error may be traced to the neglect of longer-range hopping terms in H_1 [Eq. (8)] which are themselves a consequence of the orthogonalization procedure which gave the α orbitals. For the case of two cells there are *only* nearest-neighbor interactions and we shall see in Sec. VI that in this case the fourth-order perturbation result is reproduced exactly. The important point is that the general result [Eq. (25)] remains a good approximation even when t_{pd}, t_{pp}, and ε are all of the same order. This can be seen from comparisons with exact solutions for finite clusters (see Sec. VI) and by an examination of the ratios of the matrix element for charge transfer to energy denominators. The largest ratio

$$R=\frac{|\langle \psi^s_-,0|v|\uparrow,\downarrow\rangle|}{E_- -2e_-}$$

[see Eq. (19)] is for intermediate states with two holes on the same site in the singlet state ψ^s_-. For nearest-neighbor cells this ratio is plotted in Fig. 4 as a function of ε for $t_{pp}=0$ and 0.5, with $t_{pd}=1$. We see that the ratio remains less than unity even for $\varepsilon\sim 0$, indicating convergence of the cell-perturbation expansion (though less convergent with increasing t_{pp}). By comparison, ordinary perturbation theory is hopelessly divergent in this region as can be seen in Fig. 5, where we plot the nearest-neighbor superexchange J as a function of ε, again for $t_{pp}=0$ and 0.5 and $t_{pd}=1$. In this figure the solid lines

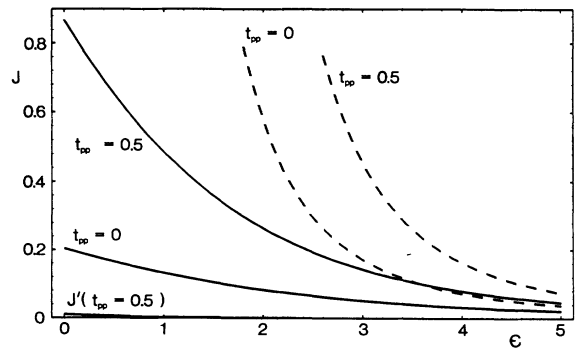

FIG. 5. Superexchange vs ε with and without direct O-O hopping. Dashed lines are the results for ordinary (fourth-order) perturbation theory [Eq. (27)].

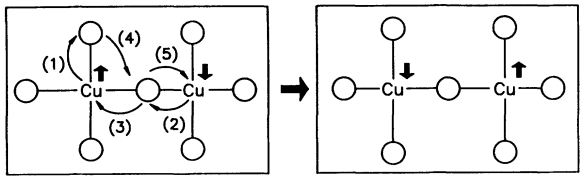

FIG. 6. A fifth-order hopping process which involves direct O-O hopping.

are plots of the general cell-perturbation result [Eq. (25)] with the results of ordinary perturbation theory [actually Eq. (27)] represented by the dashed lines. We also see from this figure that t_{pp} makes a relatively large contribution to the superexchange, particularly when the charge-transfer energy ε is small. We also include in the figure a plot of the next-nearest-neighbor superexchange J' for $t_{pp}=0.5$, which is seen to be much smaller though still appreciable for small ε. The contribution to J' due to t_{pd} is extremely small being a direct consequence of the longer-range hopping terms generated by the orthogonalization procedure.

Finally we note that Eq. (27) is similar to what we would expect from ordinary perturbation theory, with hopping processes involving t_{pp} first occurring in fifth order, i.e., fourth order in t_{pd} and first order in t_{pp}. A typical process is shown in Fig. 6.[27]

V. THE DOPED INSULATOR

When further holes are introduced into the CuO_2 plane (which is achieved by doping or a change of stochiometry in the actual materials) it becomes metallic since there is no barrier to charge transfer for sites which are doubly occupied. The effective Hamiltonian for the ground manifold is still given by Eq. (3), but P_0 will now contain states with doubly occupied sites but no unoccupied sites since these will be much higher in energy. We will also assume that the doubly occupied sites remain in the singlet ground state, ψ^s_- [see Eq. (13)] in P_0, i.e., that the other singlet and particularly the triplet are sufficiently high in energy to be accounted for perturbatively, and will therefore be in $1-P_0$. This will be justified later.

Since the singlets may hop from site to site we must add to the effective Hamiltonian for the insulating case [Eq. (16)] the first-order term

$$P_0H_1P_0=\sum_{\langle \mathbf{r},\mathbf{r}'\rangle,\sigma} t(\mathbf{r}-\mathbf{r}')[X^{\mathbf{r}}_{s,\sigma}X^{\mathbf{r}'}_{\sigma,s}+\text{H.c.}]\ , \tag{28}$$

where [see Eq. (20)]

$$t(\mathbf{r}-\mathbf{r}')=\langle \sigma,s|v(\mathbf{r}-\mathbf{r}')|s,\sigma\rangle\ , \tag{29}$$

and we have written $|\psi^s_-,\psi^\sigma_-\rangle=|s,\sigma\rangle$ for brevity. Now the Hubbard X operators interchange a two-hole singlet at one site with a single hole at an adjacent site and may thus be mapped onto a single-band kinetic-energy operator, i.e.,

$$X^{\mathbf{r}}_{s,\sigma}X^{\mathbf{r}'}_{\sigma,s}\equiv P_0c^\dagger_{\mathbf{r},-\sigma}c_{\mathbf{r}',-\sigma}P_0\ , \tag{30}$$

where P_0 ensures that we remain in the ground manifold.

Combining this with Eq. (16) the effective Hamiltonian becomes

$$H_{\text{eff}}=P_0\left[\sum_{\langle \mathbf{r},\mathbf{r}'\rangle,\sigma} t(\mathbf{r}-\mathbf{r}')(c^{\dagger}_{\mathbf{r},\sigma}c_{\mathbf{r}',\sigma}+\text{H.c.}) + \sum_{\langle \mathbf{r},\mathbf{r}'\rangle} J(\mathbf{r}-\mathbf{r}')\mathbf{s}_{\mathbf{r}}\cdot\mathbf{s}_{\mathbf{r}'}\right]P_0 , \quad (31)$$

where, of course, the Heisenberg interaction only occurs for pairs of neighboring sites which are singly occupied.

Explicit calculation of the effective single-band hopping parameters, $t(\mathbf{r}-\mathbf{r}')$, gives

$$t(\mathbf{r}-\mathbf{r}')=-\left[\tfrac{1}{2}\cos^2\phi\sin(2\theta)+\frac{1}{\sqrt{2}}\sin(2\phi)\sin^2\theta\right]\times\tau(\mathbf{r}-\mathbf{r}') - \left[\tfrac{1}{2}\cos^2\theta\cos^2\phi+\sin^2\theta\sin^2\phi + \frac{1}{2\sqrt{2}}\sin(2\phi)\sin(2\theta)\right]\tau'(\mathbf{r}-\mathbf{r}') . \quad (32)$$

These hopping parameters fall off rapidly with distance, as do the superexchange terms. We shall only retain nearest and next-nearest-neighbor terms, setting $t(|\mathbf{r}-\mathbf{r}'|=1)=t$ and $t(|\mathbf{r}-\mathbf{r}'|=\sqrt{2})=t'$, and similarly for J. Substituting into Eq. (31) gives directly the so-called t-t'-J-J' model.

As with the superexchange we can expand $t(\mathbf{r}-\mathbf{r}')$ in powers of $t_{pd}/\bar{\varepsilon}$, giving the lowest-order perturbation results

$$t(\mathbf{r}-\mathbf{r}')=-\tfrac{1}{2}\tau'(\mathbf{r}-\mathbf{r}')-\theta\tau(\mathbf{r}-\mathbf{r}') =\nu(\mathbf{r}-\mathbf{r}')t_{pp}+4\mu_0\mu(\mathbf{r}-\mathbf{r}')\frac{t_{pd}^2}{\bar{\varepsilon}} . \quad (33)$$

For nearest-neighbor hopping (t) and next-nearest-neighbor hopping (t') this gives

$$t\simeq -0.27t_{pp}-0.54\frac{t_{pd}^2}{\bar{\varepsilon}}\simeq -\frac{t_{pp}}{4}-\frac{t_{pd}^2}{2\bar{\varepsilon}} \quad (34)$$

and

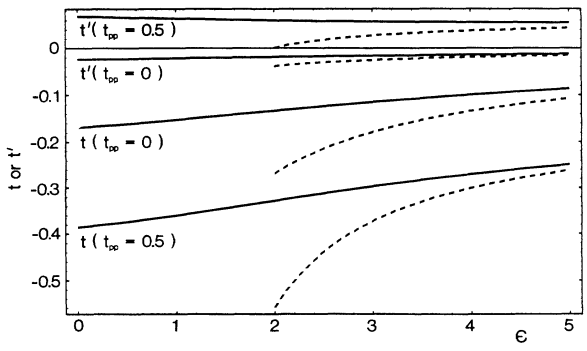

FIG. 7. Effective single-band hopping parameters for nearest-neighbors (t) and next-nearest neighbors (t') vs ε. Dashed lines are the result of ordinary (second-order) perturbation theory [Eq. (33)].

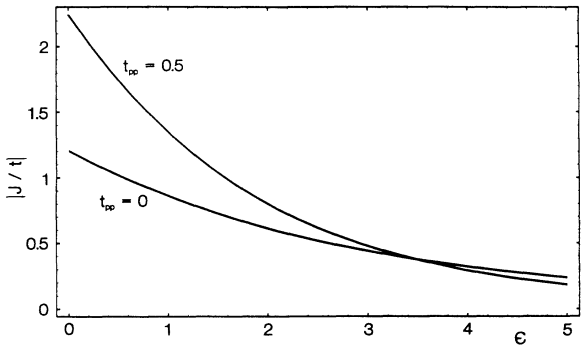

FIG. 8. Ratio of superexchange to effective single-band hopping ($|J/t|$) vs ε.

$$t'\simeq 0.12t_{pp}-0.12\frac{t_{pd}^2}{\bar{\varepsilon}}\simeq\frac{1}{8}\left[t_{pp}-\frac{t_{pd}^2}{\bar{\varepsilon}}\right] . \quad (35)$$

We see from these equations that the O-O hopping t_{pp}, makes a significant contribution to both t and t'. This is also seen in Fig. 7 where the full [Eq. (32)] and approximate [Eqs. (34) and (35)] expressions for t and t' are plotted against ε, all in units of t_{pd}. Unlike the superexchange, the curves given by the more accurate expression (32) are fairly flat and the ordinary second-order perturbation results [(34) and (35)] are not even qualitatively correct for realistic values of the parameters. Thus, since J varies quite rapidly with ε, there is an appreciable increase in the ratio $|J/t|$ as ε is decreased, as shown in Fig. 8, and $|J/t|>1$ for $\varepsilon<\sim 1.5$, increasing sharply as $\varepsilon\rightarrow 0$. This is, or course, potentially very important for the t-J model, the behavior of which is believed to depend strongly on the ratio J/t. We also note that the sign of t' changes for $t_{pp}=0$ and 0.5. This is because the contributions due to t_{pd} and t_{pp} have opposite signs and cancel for $t_{pp}/t_{pd}\sim\frac{1}{8}$. This is shown in Fig. 9 where we plot t, t',and the ratio $|t'/t|$ vs t_{pp} with $t_{pd}=1$ and $\varepsilon=2$ (the curves are similar for other values of ε). We see that both $|t'|$ and $|t|$ increase with t_{pp} but that the ratio $|t'/t|$ is only slightly greater at $t_{pp}=0.5$ than at $t_{pp}=0$. Thus,

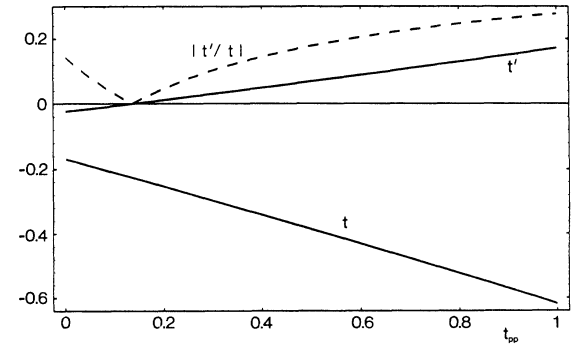

FIG. 9. Graph showing the relative variation of nearest-neighbor and next-nearest-neighbor effective single-band hopping with t_{pp}.

contrary to what might be expected, direct O-O hopping is ineffective in significantly increasing the magnitude of t' relative to t over the parameter range of interest. However, it should be noted that the change in the sign of t' can have an important effect on the hole dispersion, such as changing the positions in $\mathbf{k}$ space of the band extrema.[15]

Finally let us consider the excited states in which a pair of holes form a triplet. We have assumed that these states are sufficiently high in energy to be excluded from the ground manifold. For this assumption to be valid, i.e., in order to account for these states by perturbation theory, then the ratio $|\langle -\sigma,\psi^t_{1,2\sigma}|v|\psi^s_-,\sigma\rangle/\Delta E|$ should be small, where ΔE is the energy denominator $\bar{\varepsilon}-E_-$. Explicit calculation gives

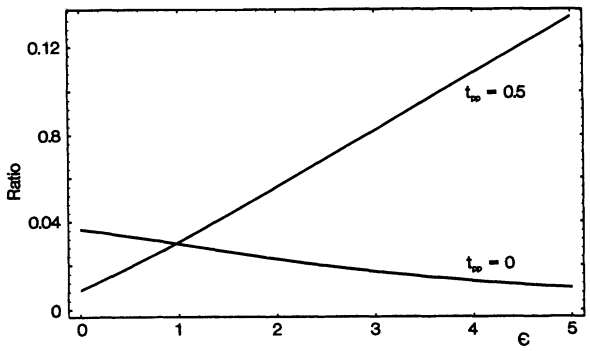

FIG. 10. Ratio of singlet-triplet transfer matrix element to energy required to make transfer (ΔE) vs ε.

$$\left|\frac{\langle -\sigma,\psi^t_{1,2\sigma}|v(\mathbf{r}-\mathbf{r}')|\psi^s_-,\sigma\rangle}{\Delta E}\right| = \frac{\tau(\mathbf{r}-\mathbf{r}')\sin^2\theta\sin\phi-\tau'(\mathbf{r}-\mathbf{r}')[(1/\sqrt{2})\cos^2\theta\cos\phi+\frac{1}{2}\sin(2\theta)\sin\phi]}{\bar{\varepsilon}-E_-} . \tag{36}$$

This ratio is plotted in Fig. 10 for nearest-neighbor cells and is always less than unity. We note that for $t_{pp}=0.5$ the ratio increases with ε. This is because the singlet-triplet splitting ΔE becomes smaller as ε increases (vanishing in the unphysical limit $\varepsilon\to\infty$) whilst the hopping matrix elements will always have a term linear in t_{pp}. Such a breakdown of perturbation theory when ε is large is also consistent with the result that the t-t'-J-J' model *cannot* be valid when $\varepsilon\to\infty$. This follows because J and J' would both be zero in this limit and we would thus have a t-t' model for the *constrained* effective single band (the Nagaoka limit). However, this cannot be the case since we know that in this limit the problem is exactly soluble because the oxygen holes completely decouple from the copper spins and we simply have an *unconstrained* oxygen band (an ordinary tight-binding band based on the α orbitals). For realistic parameters, however, the perturbation expansion converges rapidly and the singlet to triplet hopping may be accounted for as a virtual process and gives a relatively small correction to t' (see Sec. VII).

VI. COMPARISON WITH NUMERICAL RESULTS FOR FINITE CLUSTERS

The analysis of the previous sections which resulted in the t-t'-J-J' model is quite general and may be applied to finite clusters of N cells. The only difference between the various cases is the magnitude of the parameters μ and ν. In Table I these parameters are appropriate to an infinite CuO_2 sheet. In this section we shall consider clusters of just two cells in order to compare our cell-perturbation results with exact diagonalizations.

Consider first the case of Cu_2O_7 shown in Fig. 11 i.e., two CuO_4 cells with a common bridging oxygen. This case has been studied in detail in Ref. 15 in which the cluster is diagonalized exactly for realistic values of the energy parameters and the low-energy physics is shown to be described accurately by a t-J model. Here we shall again perform exact diagonalizations but with $U_d=\infty$ and $U_p=0$, comparing these results with our cell-perturbation method to investigate its accuracy when t_{pp} and ε are varied. In particular, we are interested in small ε where we expect the low-order perturbation expansions to be less accurate.

For the insulating case of just two holes in Cu_2O_7, the results of Sec. IV still apply and the low-energy physics is described by a Heisenberg Hamiltonian [cf. Eqs. (24) and (25)]. However, in this case the *pd* hybridization parameters are $\mu_0=(\sqrt{5}+\sqrt{3})/4\simeq 0.992$, $\mu_1=(\sqrt{3}-\sqrt{5})/4\simeq -0.126$, $\nu_0=\frac{14}{15}\simeq 0.9333$, and $\nu_1=-\frac{4}{15}\simeq -0.2667$. In deriving these values we did not use the general expressions in Eq. (7) directly since these would correspond to the somewhat trivial case of Cu_2O_4 with periodic boundary conditions. Rather, as with Zhang and Rice, we formed the symmetric combinations centered on each Cu

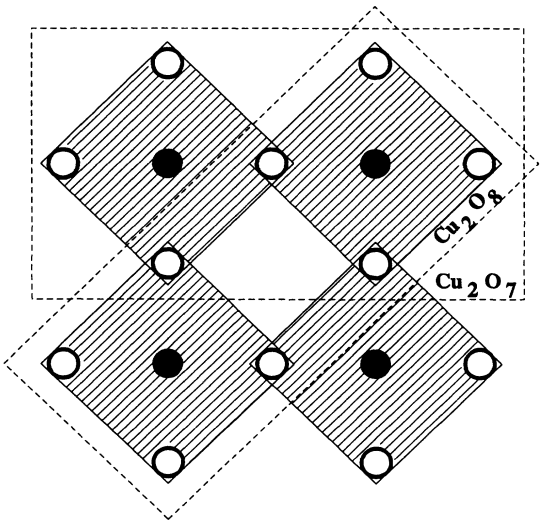

FIG. 11. Cu_2O_7 and Cu_2O_8.

site directly and orthogonalized. In the resulting Hamiltonian the antisymmetric (β) orbitals were dropped, as before. For the case $t_{pp}=0$, the superexchange in the large-ε limit becomes [cf. Eq. (26)]

$$J=\frac{256\mu_0^2\mu_1^2t_{dp}^4}{\varepsilon^3}=\frac{4t_{dp}^4}{\varepsilon^3}\ , \tag{37}$$

where, in the last step, we have used $\mu_0\mu_1=-\frac{1}{8}$ *exactly*. Thus we retrieve the usual perturbation result, as we should since for two cells there is only nearest-neighbor hopping. When ε is not very large we must use the more accurate expression (25) for the superexchange.

In Fig. 12(a) we plot J vs ε for $t_{pp}=0$ and $t_{pp}=0.5$, comparing our approximate results with exact diagonalizations (shown as a dotted line) of the Cu_2O_7 cluster. These exact diagonalizations were performed directly on the "three-band" Hamiltonian [Eq. (6)] as well as the "two-band" model with the β orbitals dropped. The differences between these two cases were extremely small, as expected, being barely perceptible on the scale of the graphs. This adds support to the argument given in Sec. III for the neglect of the β states and shows that it applies equally to small clusters. From these curves we see that our cell-perturbation method gives excellent agreement with the exact results right down to $\varepsilon=0$ for $t_{pp}=0$ and down to $\varepsilon\sim2$ for $t_{pp}=0.5$ ($t_{pd}=1$). Thus the method is a good approximation for parameters within the expected

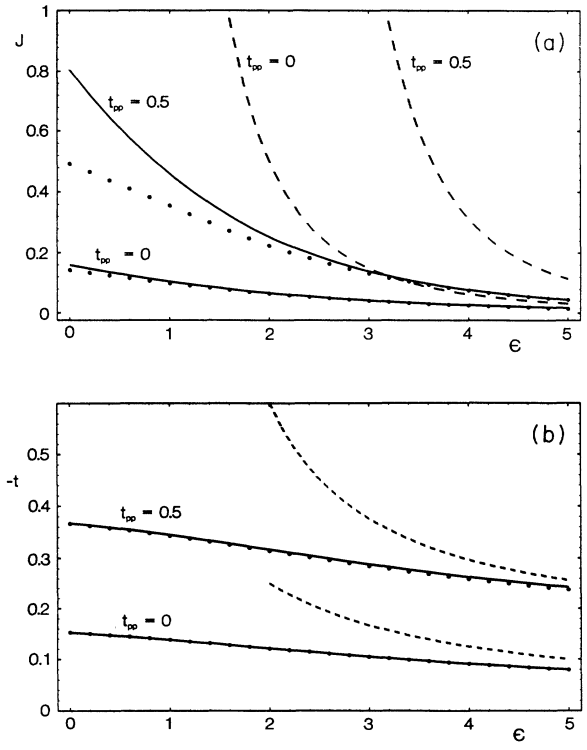

FIG. 12. Cu_2O_7. Comparison of exact results (dots) with cell-perturbation theory (solid lines). (a) Superexchange (J). (b) Effective single-band hopping ($-t$). The dashed lines are the results of ordinary perturbation theory [Eqs. (26) and (33)].

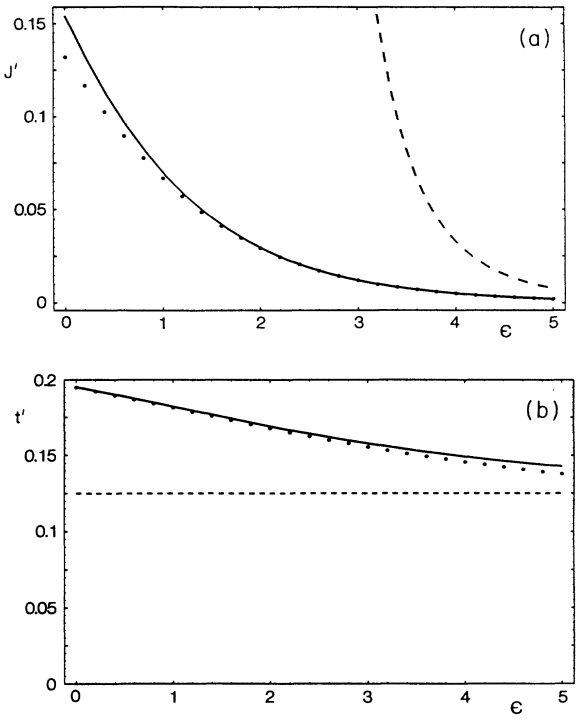

FIG. 13. Cu_2O_8. Comparison of exact results (dots) with cell-perturbation theory (solid lines). (a) Superexchange (J'). (b) Effective single-band hopping (t'). The dashed lines are the results of ordinary perturbation theory [Eqs. (26) and (33)].

range of physical interest. These results should be compared with the lowest-order expansion [Eq. (26), shown as a dashed line in Fig. 12(a)] which would result from ordinary perturbation theory. These give a very poor approximation over the full range of parameters plotted, with an error greater than a factor of 2 even for $\varepsilon=5$.

Similarly, for the "doped" case (i.e., three holes in Cu_2O_7) we show, in Fig. 12(b), plots of t vs ε for $t_{pp}=0$ and 0.5. Again we get excellent agreement with the exact results over the whole range of parameters.

In order to investigate the effective interactions for next-nearest-neighbors, i.e., t' and J', we consider the cluster Cu_2O_8. This again has been studied in detail in Ref. 15 where it is shown that the low-energy physics is accurately described by a t'-J' model. Plots of J' and t' vs ε are shown in Fig. 13 for $t_{pp}=0.5$. (Note that there is no coupling between the cells when $t_{pp}=0$.)

VII. CORRECTION TERMS

One advantage of the present method for deriving an effective Hamiltonian in a low-energy subspace is that it allows, in principle, a systematic calculation of correction terms. In this section we shall calculate two such terms and show that they are relatively small in comparison with the t-t'-J-J' terms derived earlier.

The first correction term is due to triplet states formed from two holes on a CuO_4 cell. The importance of these states has been somewhat controversial and it has been

suggested (see Ref. 17) that their proximity in energy to the singlet states may render an effective single-band model invalid. However, as we showed at the end of Sec. V, the matrix element for hopping is small compared with the singlet-triplet energy splitting and this leads to a small correction for next-nearest-neighbor hopping processes, such as the one shown in Fig. 14. The effect is merely to change t' by an amount

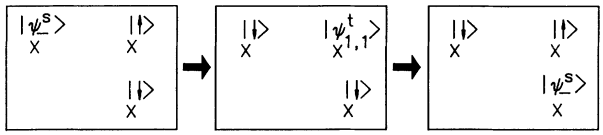

FIG. 14. Next-nearest-neighbor cell hopping via a triplet intermediate state ($X=CuO_4$ cell).

$$\delta t' = \frac{\langle -\sigma,\sigma,s|H_1|-\sigma,t,-\sigma\rangle\langle -\sigma,t,-\sigma|H_1|s,\sigma,-\sigma\rangle}{\Delta E} = \frac{\langle \sigma,s|v|t,-\sigma\rangle\langle -\sigma,t|v|s,\sigma\rangle}{\Delta E} = \frac{\{\tau_1\sin^2\theta\sin\phi-\tau_1'[(1/\sqrt{2})\cos^2\theta\cos\phi+\frac{1}{2}\sin(2\theta)\sin\phi]\}^2}{\bar{\varepsilon}-E_-}, \tag{38}$$

where v is the interaction between two neighboring cells, s is the singlet state of two holes, σ is the spin state of one hole, and t is the triplet state ($S_z=-2\sigma$) of the two holes in the intermediate state. In Fig. 15 we plot $\delta t'/t'$ vs ε for $t_{pp}=0$ and 0.5 from which we see that the correction is indeed quite small, though increasing with ε for $t_{pp}=0.5$ (due to the singlet-triplet splitting getting smaller whilst the cell-hopping matrix element tends to a constant; see the discussion at the end of Sec. V).

Note that the process shown in Fig. 14 is only allowed when sites 2 and 3 are of opposite spin though there are no such restrictions when the intermediate state is $|\psi^t_{1,0}\rangle$, for which spins 2 and 3 may be either parallel or antiparallel. In the latter case a spin flip is involved in the resulting diagonal hop of the Zhang-Rice singlet. Furthermore, it may be shown, by explicit calculation, that the corresponding matrix elements for all processes with $S_z=0$ in the triplet intermediate state are smaller by a factor $\sqrt{2}$ compared with those with $S_z=\pm 1$. Thus the corrections to next-nearest-neighbor hopping do not simply renormalize t' but depend in magnitude on the local spin configuration and can involve spin flips. It should be noted that similar next-nearest-neighbor hopping terms (including spin flips) also arise when the t-J model is derived from the single-band Hubbard model. However, these always involve *singlet* intermediate states as shown, for example, in Fig. 16. Similar processes are also allowed here but we point out that such corrections are *much smaller* than those involving triplet intermediate states (due to high intermediate-state energies of the singlets) and, as pointed out by Emery and Reiter,[17] it is the triplet states, which give rise to the most important corrections. Although these corrections are quite small relative to t', they may well be comparable with J (depending on parameters) and may thus have a significant effect on charge motion.[28,29] Nevertheless, this does not invalidate an effective single-band description and the correction terms in the effective Hamiltonian may be accurately computed as described above.

The other correction term we will consider is the interaction between pairs of holes on neighboring cells. These are of potential importance for superconductivity since if such an interaction were attractive it could be a source of pairing. We will, in fact, show that the interaction is indeed attractive, though very small. The question as to how this might contribute to Cooper pairing and superconductivity is a very difficult one and will not be considered further in this paper. We merely point out that this attraction between singlets on neighboring cells can be thought of as an attraction between the underlying oxygen holes, which move in a background of static (Cu) spins and that such a small attractive interaction will almost certainly be swamped by kinetic-energy (hopping) terms which would mitigate against pairing.[30]

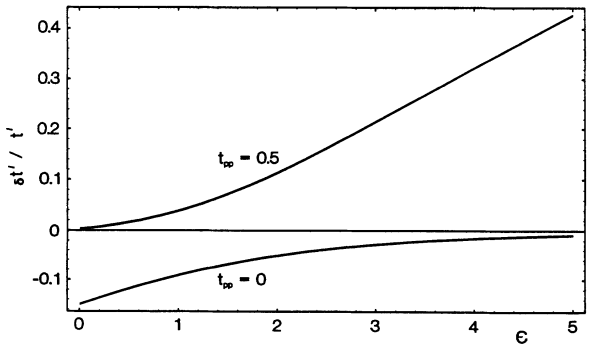

FIG. 15. Relative correction to next-nearest-neighbor hopping ($\delta t'/t'$) via a triplet intermediate state, with and without direct O-O hopping.

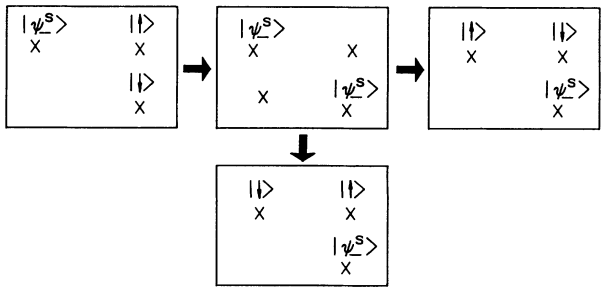

FIG. 16. Other (less important) next-nearest-neighbor hopping processes which also occur in the single-band Hubbard model ($X=$ CuO_4 cell).

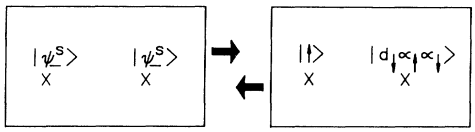

FIG. 17. Hole-hole attraction process which occurs for neighboring cells that are doubly occupied.

In Fig. 17 we show two neighboring cells which are doubly occupied with holes, each cell being in its lowest singlet ground state. Interaction between the cells may again be calculated by second-order perturbation theory giving rise to a term in the effective single-band Hamiltonian

$$H_{\text{pair}} = -\Delta P_0 \left[\sum_{\langle r,r' \rangle} (n_r - 1)(n_{r'} - 1) \right] P_0 , \tag{39}$$

where

$$\Delta = \sum_i \frac{\langle i|v|s,s\rangle^2}{E_i - E_0} = \frac{4}{2(\bar{\varepsilon} - E_-) + e_-} M^2 \tag{40}$$

and

$$M = \langle i|v|s,s\rangle = \tau_1[2^{-3/2}\cos\theta \sin(2\phi) + \sin\theta(1 - \tfrac{3}{2}\cos^2\phi)] + \tau_1'[\tfrac{1}{2}\cos\theta\cos^2\phi - 2^{-3/2}\sin\theta\sin(2\phi)] . \tag{41}$$

This matrix element is the same for all four intermediate states corresponding to one hole on one cell (in the state $|e_-\rangle$) and three holes in the other cell (in the state $|d_\sigma \alpha_\uparrow \alpha_\downarrow\rangle$).

In Fig. 18 we plot Δ vs ε again for $t_{pp} = 0$ and 0.5 with $t_{pd} = 1$. We see that this is indeed a small energy compared with other effective interactions.

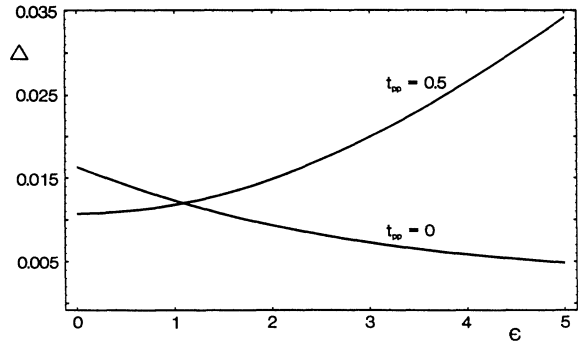

FIG. 18. Hole-hole attraction potential for neighboring cells which are doubly occupied.

VIII. DISCUSSION AND SUMMARY

A comparison of the graphs for nearest-neighbor superexchange and effective hopping for the infinite plane (Figs. 5 and 7) and for the two-cell cluster Cu_2O_7 (Fig. 12) shows that the magnitude of these quantities is always slightly larger for the infinite plane. This may be expected since the holes can increase their kinetic energy in the infinite plane. This is reflected in the delocalization of the Wannier functions and a corresponding increase in the parameters μ_1 and ν_1 characterizing nearest-neighbor cell interactions. What is less obvious is that the magnitude of the next-nearest-neighbor hopping t' is significantly smaller for the infinite plane than for the two-cell cluster Cu_2O_8. The main reason for this difference is that there is no contribution to t' from the pd interaction for the case of Cu_2O_8, i.e., $\mu_2 = 0$, whereas for the infinite plane the pd interaction makes a finite contribution which partially cancels the contribution due to O-O hopping [since μ_2 are ν_2 are of opposite signs, see Eq. (32) and Table I]. This can also be seen in Fig. 9, which shows that t' changes sign as t_{pp} is increased from zero, vanishing at $t_{pp} \simeq 0.15 t_{pd}$.

A further quantitative difference between the two-cell case and the infinite plane is the size of the correction $\delta t'$ due to triplet intermediate states (see Figs. 14 and 15). For Cu_2O_8 the correction due to triplet states is very small, especially for small ε, as can be seen by comparing the exact results with the second-order cell-perturbation result [see Fig. 13(b)]. On the other hand, for the infinite plane the corresponding correction is quite appreciable ($\sim 10\%$ or more depending on ε). The reason for this apparent discrepancy is because the process shown in Fig. 14 is not allowed for Cu_2O_8. However, let us again emphasize that although these triplet states give the largest correction for the infinite plane, they can be accounted for quite satisfactorily by perturbation theory where they appear as intermediate states and an effective single-band description remains valid. We can in principle, of course, generate a more accurate single-band effective Hamiltonian with longer-range interactions by going to higher orders in perturbation theory, though such corrections are expected to be relatively small due to the smallness of the expansion parameters (see, for example, Figs. 4 and 10).

Finally, let us briefly consider the insulator-metal (IM) transition which must occur when the "bare" charge-transfer energy ε becomes sufficiently small. Now the perturbation method used in this paper is convergent right down to $\varepsilon = 0$ where the second-order approximation remains fairly good. Although this implies that the Heisenberg model will yield good estimates of the true low-lying eigenstates, even for $\varepsilon = 0$, it does not prove that the model will remain insulating as may be seen from the following argument. Consider a plane with a large number of cells, $2N$, with the number of holes equal to the number of cells. If we consider the manifold of states with exactly one hole per cell then the analysis of Sec. IV shows that the eigenstates emanating from these base states are given by a Heisenberg model. We now consider a set of states in which a hole is transferred from one-half of the plane to the other. Thus one-half of the plane has

$N-1$ cells singly occupied with holes and one cell unoccupied, whereas the other half will have a doubly occupied cell with the remainder singly occupied. Relative to the states with one hole per cell the unoccuppied cell contains an electron, whereas the doubly occupied site contains an (extra) hole. We shall refer to these extra charges as *the* electron and hole. Now in the limit that N becomes infinitely large we may regard the two halves of the plane as independent as regards the motion of the electron in one-half and the hole in the other. According to the results of Sec. V we may describe the motion of the hole by a t-t'-J-J' model and there will be similar effective single-band model describing the motion of the electron. Let the ground-state energies for these "t-J" Hamiltonians with N cells be $E_0^{(1)}$ and $E_0^{(2)}$ for the electron and hole, respectively, and let the ground-state energy of the Heisenberg model with $2N$ cells be E_0. Then the true energy to make a charge transfer taking into account the kinetic energies of the electron and hole is $\Delta E=E_0^{(1)}+E_0^{(2)}-E_0$ and an IM transition will take place when $\Delta E=0$. In order to determine precisely where this transition will occur requires exact solutions of the Heisenberg and t-J models, but these are not presently available and even approximate solutions are unreliable. However, we point out that if accurate solutions do become available the critical region in parameter space $(\varepsilon,t_{pd},t_{pp})$ for an IM transition should also be calculable to high accuracy. (Note that this is not the case for the single-band Hubbard model which is approximately equivalent to a t-J model only in the region $J=4t^2/U \ll t$, i.e., $t \ll U$. However, the IM transition occurs for $t \sim U$ where a low-order perturbation expansion in t/U is invalid.) In the absence of accurate solutions of the effective single-band models let us make a crude (over)estimate of the critical ε for the IM transition with $t_{pd}/t_{pp}=2$. To do this we cut the perturbation expansions off at first order. This gives $E_0=2N\varepsilon_-$, $E_0^{(1)}=(N-1)\varepsilon_-+\varepsilon_e$, and $E_0^{(2)}=(N-1)\varepsilon_-+\varepsilon_h$, i.e., $\Delta E=\varepsilon_e+\varepsilon_h-2\varepsilon_-$, where ε_e and ε_h are the minimum energies of the electron and hole performing their band motion. Note that there are no J dependencies in these expressions as they are only to first order. Since these (charge-spin) interactions inhibit charge motion we are thus overestimating the kinetic energies of the electron and hole. We shall further simplify the problem by just using the simple nearest-neighbor tight-binding expressions for a free electron and hole which again gives a greater kinetic energy than with the constrained motion.[31] Thus we get $\Delta E=E_- -4(|t_e|+|t_h|)-2\varepsilon_-$ where $t_h=t$ is given by Eq. (32) and, by explicit calculation for the effective electron hopping, $t_e=\tau_1\sin(2\theta)+\tau_1'\sin^2\theta$. Solving $\Delta E=0$ gives the IM transition at $\varepsilon/t_{pd}=2.79$. This is remarkably close to what has been obtained by Grilli *et al.* in a mean-field slave boson theory for the d-p model, in which charge-spin interactions were also ignored.[32] However, we do emphasize that this rather crude overestimate of the critical charge-transfer gap could be substantially reduced if proper account were made of the reduction in mobility of the electron and hole due to charge-spin interactions.

The main results of this paper may be summarized as follows.

(i) An effective single-band model accurately describes the low-energy states of Cu-O planes for charge concentrations (doping) close to the insulating phase. The effective single-band parameters may be derived in terms of the underlying d-p parameters using a cell-perturbation method.

(ii) O-O hopping enhances all the effective single-band parameters with the enhancement of the superexchange greatest, particularly for small (bare) charge-transfer energies. For realistic values of the d-p parameters the superexchange and hopping terms are expected to be comparable $(0.3<J/t<1)$.

(iii) The largest corrections are due to triplet states though these may be accounted for by perturbation theory where they appear as intermediate states. They include three site terms similar to those which arise in the derivation of the t-J model from the Hubbard model but occur for quite different reasons and may be somewhat larger in magnitude. Other corrections, such as hole-hole attraction terms, are much smaller.

(iv) An upper limit on the critical (bare) charge-transfer energy for an insulator-metal transition is $\varepsilon=2.79$ for $t_{pp}=\frac{1}{2}$ (in units of t_{pd}). This could be substantially reduced by charge-spin interactions.

(v) Our cell-perturbation expansion is highly convergent and the second-order result remains a good approximation even in the parameter range where $J \sim t$. This would not be the case for the single-band Hubbard model, of course, which only approximates to a t-J model when $J \ll t$.

The above conclusions may no longer be valid when further orbitals in the d-p model are considered and the effect of apical oxygen ions taken into account. Indeed there is some evidence that this may lead to further low-energy states which become degenerate, or nearly so, with the Zhang-Rice singlets, rendering an effective single-band description inadequate.[33–37] We hope to discuss these cases in more detail in a forthcoming publication.

ACKNOWLEDGMENTS

We thank C. DiCastro, S. Sarkar, and G. Sawatzky for stimulating discussions. This investigation was supported by the European Community under the SCIENCE program for collaborative research (Contract No. SCI-0222-C).

[1] P. W. Anderson, Science **235**, 1196 (1987); P. W. Anderson, *Frontiers and Borderlines in Many Particle Physics,* edited by J. R. Schrieffer and R. A. Broglia, International School of Physics "Enrico Fermi," Varenna, 1987 (North-Holland, Amsterdam, 1989).

[2] Strictly speaking, there are second-order next-nearest-neighbor hopping terms of order J, though these are often omitted. See, for example, S. A. Trugman, Phys. Rev. B **41**, 892 (1990).

[3]V. J. Emery, Phys. Rev. Lett. **58**, 2794 (1987).
[4]G. van der Laan, Solid State Commun. **42**, 165 (1982).
[5]A. Fujimori, Phys. Rev. B **39**, 793 (1989).
[6]K. Okada and A. Kotani, J. Electron Spectrosc. Relat. Phenom. **52**, 313 (1990).
[7]H. Eskes, L. H. Tjeng, and G. A. Sawatzky, Phys. Rev. B **41**, 288 (1990).
[8]O. Gunnarsson *et al.*, Phys. Rev. B **41**, 4811 (1990).
[9]C. T. Chen *et al.*, Phys. Rev. Lett. **66**, 104 (1991).
[10]M. S. Hybertsen, M. Schlüter, and N. E. Christensen, Phys. Rev. B **39**, 9028 (1989).
[11]A. K. McMahan, R. M. Martin, and S. Satpathy, Phys. Rev. B **38**, 6650 (1988).
[12]J. H. Jefferson, J. Phys. Condens. Matter **1**, 1621 (1989).
[13]F. C. Zhang and T. M. Rice, Phys. Rev. B **37**, 3757 (1988).
[14]H. Eskes and G. A. Sawatzky, Phys. Rev. Lett. **61**, 1415 (1988).
[15]H. Eskes, G. A. Sawatzky, and L. F. Feiner, Physica C **160**, 424 (1989).
[16]M. S. Hybertsen, E. B. Stechel, M. Schlüter, and D. R. Jennison, Phys. Rev. B **41**, 11 068 (1990).
[17]V. J. Emergy and G. Reiter, Phys. Rev. B **38**, 4547 (1988).
[18]J. H. Jefferson, Physica B **165&166**, 1013 (1990).
[19]J. Hubbard, Proc. R. Soc. A **277**, 237 (1964).
[20]S. T. Chui and J. W. Bray, Phys. Rev. B **18**, 2426 (1978).
[21]K. W. H. Stevens, Phys. Rep. **24**, 1 (1976).
[22]D. J. Newman, J. Phys. Chem. Solids **31**, 1143 (1970).
[23]C. Bloch, Nucl. Phys. **6**, 329 (1958).
[24]I. Lindgren and J. Morrison, *Atomic Many-Body Theory* (Springer, Berlin, 1986).
[25]B. S. Shastry, Phys. Rev. Lett. **63**, 1288 (1989).
[26]P. W. Anderson, Phys. Rev. **115**, 2 (1959).
[27]The equivalence is not quite correct when $t_{pp} \neq 0$ since ordinary perturbation theory would be in powers of t_{pd}/ε and t_{pp}/ε, whereas Eq. (27) involves the "renormalized" energy $\bar{\varepsilon} = \varepsilon - 2\nu_0 t_{pp}$. Thus our (more accurate) Taylor expansion is equivalent to summing a subclass of terms to infinite order.
[28]W. Stephan and P. Horsch (unpublished).
[29]A. Auerbach and B. E. Larson, Phys. Rev. Lett. **66**, 2262 (1991).
[30]A simple example of a small attractive interaction being insufficient to overcome kinetic effects is the single-band Hubbard model with just two electrons, which may be solved exactly. Although a second-order perturbation calculation would give rise to an attractive interaction between electrons of opposite spin on adjacent lattice sites, the exact solution shows that the ground state is unbound for all $U \geq 0$.
[31]W. F. Brinkman and T. M. Rice, Phys. Rev. B **2**, 1324 (1970).
[32]M. Grilli, G. Kotliar,and A. J. Millis, Phys. Rev. B **42**, 329 (1990).
[33]H. Kamimura, Jpn. J. Appl. Phys. **26**, L627 (1987).
[34]H. Eskes and G. A. Sawatzky, Phys. Rev. B **44**, 9656 (1991).
[35]J. B. Grant and A. K. McMahan, Phys. Rev. Lett. **66**, 488 (1991).
[36]Y. Ohta, T. Tohyama, and S. Maekawa, Phys. Rev. B **43**, 2968 (1991).
[37]C. DiCastro, L. F. Feiner, and M. Grilli, Phys. Rev. Lett. **66**, 3209 (1991).